LIMNOLOGY
and
OCEANOGRAPHY

ASLO

Limnol. Oceanogr. 63, 2018, 1911–1923

doi: 10.1002/lno.10815

Nitrogen fixation rates diagnosed from diurnal changes in elemental stoichiometry

Christopher L. Follett,[1]* **Angelicque E. White**,[2] **Samuel T. Wilson**,[3] **Michael J. Follows**[1]

[1]Department of Earth, Atmospheric and Planetary Sciences, Massachusetts Institute of Technology, Cambridge, Massachusetts

[2]College of Earth, Ocean, and Atmospheric Sciences, Oregon State University, Corvallis, Oregon

[3]Daniel K. Inouye Center for Microbial Oceanography: Research and Education, University of Hawai'i at Mānoa, Honolulu, Hawai'i

Abstract

The carbon, nitrogen, and phosphorus (C, N, and P, respectively) composition and elemental ratios were measured in the 20–200 μm size fraction during July 2015 in the surface waters of an anticyclonic eddy encountered north of Hawaii in the oligotrophic North Pacific Subtropical Gyre. The observed particulate N : P ratio fluctuated by approximately a factor of two over the diel cycle. We present a simple mathematical argument connecting this change to a rate of biological nitrogen fixation, and calculate the nitrogen fixation rate to be ≥ 13 nmol L^{-1} d^{-1} for this size class. This value is higher than simultaneous bottle-incubation based rates measured with isotopic tracers, yet is consistent with historic rate measurements from the region. As confirmation of our methods, diurnal changes in C : N : P of laboratory cultures of the diazotrophic genus *Trichodesmium* were measured. In the laboratory, we show that estimates of nitrogen fixation from stoichiometric time series are equivalent to those derived directly from mass balance. The disparity between nitrogen fixation rates derived from tracer measurements and particulate stoichiometry in the field suggests that large diazotrophs may be underestimated in small volume ($\sim$ 4 L) bottle incubations as a result of either spatial heterogeneity or vertical migration of large cells. Otherwise, processes other than diazotrophy must cause the observed changes in stoichiometry. This approach represents a novel and scalable means of quantifying in situ nitrogen fixation rates from diurnal changes in size-fractionated stoichiometry. We also infer carbon fixation, growth rates, and phosphorus uptake in the 20–200 μm size class.

Nitrogen fixation is a significant component of new production and hence carbon export, particularly in nitrogen (N) limited oligotrophic ocean regimes (Karl et al. 1997; Capone et al. 2005; Karl et al. 2012). In the North Pacific Subtropical Gyre (NPSG), nitrogen fixing phytoplankton including species of the genus *Trichodesmium* and symbioses of diatoms and the diazotroph *Richelia* (e.g., diatom-diazotroph associations [DDAs]) are estimated to contribute up to half of the annual carbon (C) and nitrogen export in this region (Karl et al. 2012; Böttjer et al. 2017). Standard methods for direct measurements of nitrogen fixation rates either use stable isotope tracer approaches ($^{15}N_2$) (Montoya et al. 1996) or quantify the reduction of acetylene gas to ethylene (Capone 1993; Wilson et al. 2012). These methods are both subject to bottle effects which may introduce artifacts such as nutrient or metal contamination or alter trophic interactions. Additionally, methodological concerns have recently been raised for the $^{15}N_2$ tracer method such that additional corrections for $^{15}N_2$ gas dissolution and potential $^{15}NH_4^+$ contamination need to be made (Mohr et al. 2010; Dabundo et al. 2014; Böttjer et al. 2017).

Biogeochemical rates can also be effectively estimated from noninvasive in situ measurements if sufficient changes exist relative to the inherent spatial variability of the variable in question. This approach has been used to estimate community production from the diel change in optically derived particulate carbon (PC), which reflects net particle growth during the day and net particle loss at night (Stramska and Dickey 1992; Walsh et al. 1995; Claustre et al. 2007; White et al. 2017). The diel cycle of nitrate has also been used to diagnose new production (Johnson et al. 2006) and

*Correspondence: follett@mit.edu

growth rates of specific planktonic groups have been estimated from diurnal changes in their cell size (Olson et al. 2003; Sosik et al. 2003; Lomas et al. 2011; Hunter-Cevera et al. 2014; McInnes et al. 2014; Ribalet et al. 2015). Each of these approaches is based on the tight relationships between growth, nutrient uptake, cell division, respiration, and light over the diurnal cycle. These methods have a different set of experimental challenges and so provide a great complement to bottle based measurements.

Here, we propose that the diel cycle of size-fractionated elemental stoichiometry can be used to diagnose nitrogen fixation rates for large-cell sized diazotrophs. This follows from the fact that two of the major classes of known diazotrophs in oligotrophic regions such as the NPSG, e.g., the filamentous heterocyst-forming *Richelia* spp. and *Calothrix* spp. which are symbionts of large diatoms (DDAs) and colony-forming spp. of the genus *Trichodesmium*, occupy a distinctive size niche (> 20 μm). Moreover, both of these genera fix nitrogen only during the daylight hours (Zehr 2011) such that particulate N increases due to diazotrophy in these size classes can only occur during the photoperiod. Other, small-cell sized diazotrophs, such as *Crocosphaera* and group A cyanobacteria (UCYN-A) exist in this system (Zehr 2011; Wilson et al. 2017), but are less than 5 μm and should not be collected by our sampling methods. In non-diazotrophs, carbon fixation leads to clear diurnal fluctuations in the C : P ratio as carbon fixation outpaces phosphorus uptake (Terry et al. 1985; Geider and LaRoche 2002; Lopez et al. 2016). The C : P ratio of these organisms is largest during the day when carbon fixation is also maximized, while available data suggests that the N : P ratio remains constant (Lopez et al. 2016).

We suggest that the N : P ratio of diazotrophs which fix nitrogen during daylight hours should similarly be maximized during the day and that this change can be used to estimate nitrogen fixation. We provide careful justification for a straightforward mass balance argument. If we know the average amount of phosphorus, $\langle P \rangle$, over the diel cycle, and we measure a change in the N : P ratio, $\Delta \frac{N}{P}$, then the flux of nitrogen can be expressed as:

$$\Delta N \approx \langle P \rangle \Delta \frac{N}{P}. \quad (1)$$

We will use this argument to estimate nitrogen fixation from diurnal time series of particulate stoichiometry measured in situ. This basic argument will be extended to estimate other quantities like growth rate and carbon fixation. We will then show that this technique holds for laboratory cultures of nitrogen fixing organisms, where the nitrogen fixation rate can be unequivocally determined from changes in particulate nitrogen (PN). Our estimates are consistent with previously measured rates, cell counts, and concentration data. Finally, we will compare our diel time series estimates with $^{15}N_2$ tracer-based measurements of nitrogen fixation in whole seawater. We have focused our work in the well-characterized NPSG where N_2 fixation rates are significant (with blooms having rates up to 25 nmol L^{-1} d^{-1}, Fong et al. 2008) and on the 20–200 μm size class as this is the size range generally encompassing large diazotrophs including DDAs and *Trichodesmium* spp. (Fong et al. 2008; Karl and Church 2014).

Methods

Field data collection

All samples were collected aboard the R/V *KOK* or R/V *Kilo Moana* between 24th July 2015 and 6th August 2015, in conjunction with the SCOPE (Simons Collaboration on Ocean Processes and Ecology) field campaign in the NPSG. These cruises targeted an anticyclonic eddy near station ALOHA (A Long-Term Oligotrophic Habitat Assessment, at 22.45°N, 158°W (Karl and Church 2014)). Sampling was conducted in a Lagrangian fashion whereby both research vessels followed a set of Surface Velocity Program (SVP) drifters to study microbial metabolism over diel timescales. The uncontaminated seawater line on the R/V *KOK* supplied water from approximately 7 m below the waterline of the ship's bow. This source water was pre-filtered through 200 μm Nitex mesh in order to exclude grazers. This mesh also excludes large colonies of nitrogen fixers, but, at least for *Trichodesmium*, this effect is expected to be small ($\sim$ 6% of the total; White et al. 2018). Water was then fed through a plankton net with 20 μm mesh net and cod-end. Volume filtered was recorded by measuring the flow rate over the filtration interval using an in-line flow meter. Over 1000 L of water per sample was filtered in this manner in order to ensure a sufficient signal to noise ratio for PC, PN, and particulate phosphorus (PP). This process was repeated every 2 h (for periods of approximately 20 h), over the course of multiple diel cycles with a few smaller runs interspersed (7/26, 7/27–7/28, 7/29–7/30, 7/31, 8/1–8/2). In this context, a run refers to a set of samples taken every 2 h without any breaks. The taxonomic composition of the 20–200 μm size class was examined near the end of the time series via light microscopy (*see* Fig. 1).

At the end of the filtration period, the contents of the 20 μm mesh cod-end, which we will refer to as the concentrate, was vacuum filtered onto GF/F filters in series, with half of the volume filtered onto pre-combusted GF/F for PC and PN and the other half of the volume filtered onto acid-washed and combusted GF/F for analysis of PP. All filters were frozen at -20°C until later analysis at the University of Hawaii using standard methods from the Hawaii Ocean time series (HOT) program (Karl and Lukas 1996; Karl and Church 2014). The first time point for each time series section ($n = 4$ samples) was excluded from the analysis because the mean values were always substantially higher than the mean of samples collected at the next time point, independent of the time of day the data collection run began. Additionally, small samples (200 mL splits), of water which had passed

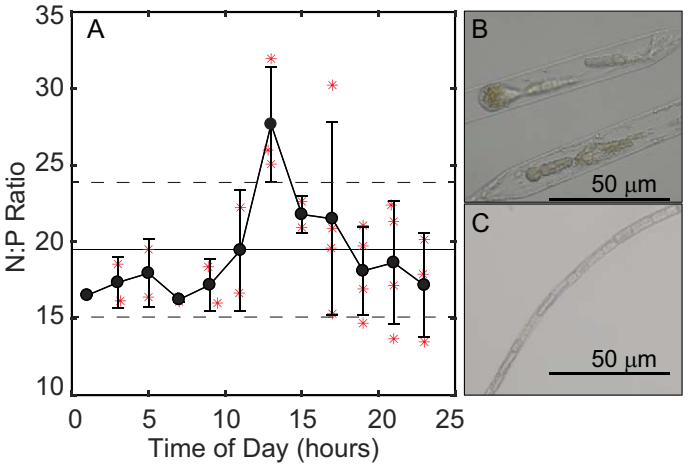

Fig. 1. Large diazotrophs exhibit diurnal fluctuations in elemental stoichiometry. (**A**) The ratio of nitrogen to phosphorus (N : P) in the size class containing large diazotrophs fluctuates diurnally as nitrogen fixation rates exceed net phosphorus uptake near the solar zenith (*see* "Results" section). Individual measurements (stars) are averaged in 2 h windows (black circles). Horizontal lines are the mean and standard deviation intervals for the entire data set. (**B**, **C**) Micrographs of representative diazotrophs observed near Station ALOHA in July 2015. (**B**) During this cruise, *Rhizosolenia* sp. containing *Richelia* sp. were found to be the most abundant DDA although *Chaetoceros* sp. and *Hemialus* sp. DDAs were also present. (**C**) *Trichodesmium* was also observed albeit at lower concentrations than DDAs. [Color figure can be viewed at wileyonlinelibrary.com]

through the net filter were filtered onto GF/F at four time points to act as blanks. The average of these values, representing 7% ± 3%, 8% ± 4%, and 2% ± 0.3% of the PC, PN, and PP signal, was subtracted from each filter value before the bulk concentrations and ratios were calculated.

Samples were also collected (R/V *Kilo Moana*) for microscopic enumeration of large diazotrophs present during the field campaign. At select stations and depths (ranging from 5 m to 45 m), the entire volume of a Niskin bottle was drained directly into clean 10 L carboys fitted with spigots for enumeration of large diazotrophs. Carboys were covered in dark cloth and the volume was gravity filtered through a 47-mm diameter, 10 μm pore size, black polycarbonate filter with a polyester drain disk as a backing filter. Filtration time was always less than 2 h. Following filtration, filter holders were fit with a short section of tubing and a syringe luer fitting on one side, and a two-way valve on the outflow side. For each filter, 5-mL of 2% glutaraldehyde was slowly injected onto the filter and samples were allowed to fix for 30 min. Fixative was drained after this time and 60 mL of air was used to flush all filters. Polycarbonate filters were then mounted onto glass slides with immersion oil, cover slides were added and the edges of each cover slip were sealed with quick dry nail polish. All slides were stored at −20°C until enumeration of diazotrophic taxa using epifluorescence microscopy. The entire slide was counted for *Trichodesmium* spp. abundance and for endosymbiont-bearing diatoms as well as free *Richelia intracellularis*. *Trichodesmium* filaments were counted, and the length of each filament was recorded. *Trichodesmium* cell number was then calculated by dividing the filament length by the mean cell length (12 ± 2 μm). *Richelia* and *Calothrix* heterocysts rather than vegetative cells were counted and results are expressed as *Richelia* for simplicity.

Time series of nitrogen fixation were also estimated via measurement of $^{15}N_2$ assimilation in bottle incubations (Wilson et al. 2017). Rates of $^{15}N_2$ assimilation were conducted using ^{15}N-labeled gas (Cambridge Isotope Laboratories) dissolved in filtered seawater prior to its addition. The quantities of nitrogen isotopes (i.e., N masses equivalent to 28, 29, and 30) were measured in each batch of $^{15}N_2$ enriched seawater (Böttjer et al. 2017) and the final atom % enrichment in the seawater incubations averaged 5.7 ± 0.5. Two hundred milliliters of $^{15}N_2$-enriched seawater was added to a 4 L polycarbonate bottle which had been filled from a depth of 15 m. Rates of N_2 fixation were measured in triplicate with a 4 h incubation period during 27–30 July 2015 and 31 July–03 August 2015. Samples were incubated using on-deck incubators shaded to a light level equivalent of 15 m and maintained at near in situ temperatures. After the incubation period, the entire contents of the 4 L bottle were filtered via a peristaltic pump onto a pre-combusted glass microfiber (Whatman 25 mm GF/F) filter and stored at −20°C. On land, the filters were analyzed for the total mass of N and the $\delta^{15}N$ composition using an elemental analyzer-isotope ratio mass spectrometer (Carlo-Erba EA NC2500 coupled with Thermo-Finnigan Delta S) at the Stable Isotope Facility, University of Hawaii.

Laboratory experiments

Batch cultures of *Trichodesmium* IMS101 were monitored over two consecutive diel cycles during exponential growth at Oregon State University. This strain was originally isolated from coastal Atlantic waters (Prufert-Bebout et al. 1993) and has since been identified as *Trichodesmium erythraeum* (Janson et al. 1999). Cultured populations were maintained on an artificial seawater medium (YBCII) lacking combined nitrogen (N) sources as described by Chen et al. (1996) with an initial dissolved inorganic phosphorus concentration of 5 μmol L^{-1}. Cultures were maintained at 24°C in a computer-controlled incubator with cool white fluorescent lights set on a 12/12 square light–dark cycle with a noon maximum of 500 μmol quanta m^2 s^{-1}. Over a 2-d period, duplicate batch cultures were sampled at 2-h intervals during the light cycle for PC, PN, and PP and acetylene reduction as per the methods described in White et al. (2010). Briefly, PP concentrations were measured spectrophotometrically as dissolved phosphate following combustion (450°C, 5 h) and acid hydrolysis (0.15M HCl, 60 min at 60°C) according to the method of Karl et al. (1991). PC and PN were analyzed on a Carlo Erba elemental analyzer (model NA1500) using

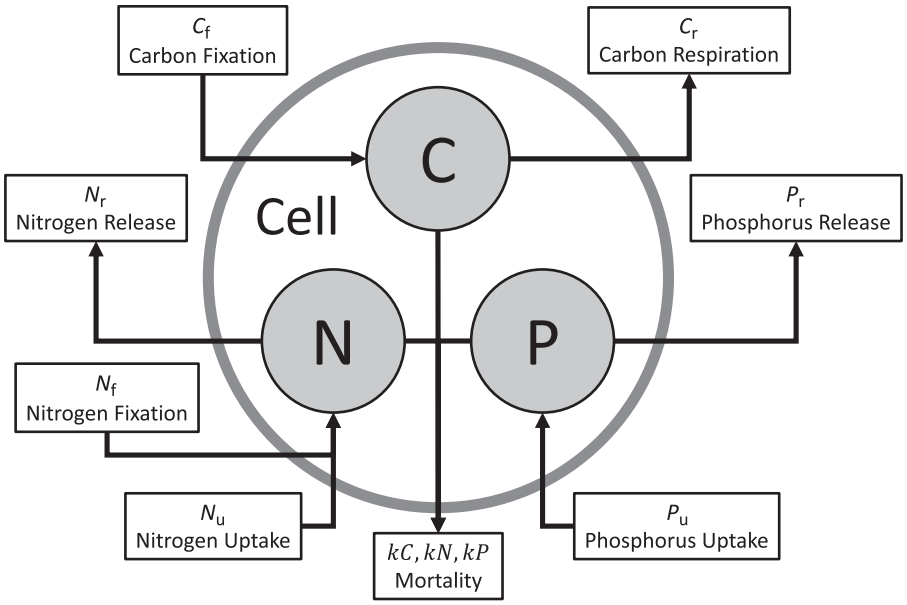

Fig. 2. Particulate mass balance: this schematic shows all of the elemental fluxes into and out of cellular material represented by our differential equations.

acetanilide (71.09% C and 10.36% N by weight) as the primary standard.

Equating stoichiometric fluctuations with rates

Here, we generate a set of equations to relate the diel fluctuations in particulate organic carbon (C), nitrogen (N), and phosphorus (P) concentrations (μM) to biogeochemical transformation rates. In the following section, we apply these equations first to our data for the 20–200 μm size fraction, and then to experimental cultures of *Trichodesmium*. We model the evolution of PN, PP, and PC with a set of differential equations

$$\frac{dN}{dt} = N_f + N_u - N_r - kN \tag{2}$$

$$\frac{dP}{dt} = P_u - P_r - kP \tag{3}$$

$$\frac{dC}{dt} = C_f - C_r - kC \tag{4}$$

where N_f is the time dependent nitrogen fixation rate, N_u is the time dependent uptake rate, and N_r is the release rate. For phosphorus, P_u is the phosphate uptake rate and P_r its release rate. For carbon, C_f is the carbon fixation rate and C_r is the sum of respiration and organic carbon release. k is the death rate and affects all elements equally. All of these rates can have time dependence. These fluxes are illustrated in Fig. 2.

We then reframe these equations in terms of fluctuations in stoichiometric ratios, specifically the ratio of N : P,

$$N_p = \frac{N}{P}. \tag{5}$$

This is done to account for physically caused fluctuations in the absolute concentrations (Sosik et al. 2003), as well as errors in the measurements themselves. In order to equate changes in N : P to a nitrogen fixation rate, we will assume that all increases in the N : P ratio are caused by nitrogen fixation. Mechanistically, this means two things. First, rates of nitrogen uptake do not exceed phosphorus uptake relative to the current N : P ratio. Second, phosphorus release by cells must be accompanied by commensurate nitrogen release. We analyze the validity of these assumptions in the context of our field site and data in the discussion section.

Nitrogen fixation rate

Defining the ratio of nitrogen to phosphorus, $N_p = \frac{N}{P}$, as in Eq. 5, we can write the derivative of the ratio using the quotient rule as

$$\frac{dN_p}{dt} = \frac{P\frac{dN}{dt} - N\frac{dP}{dt}}{P^2}. \tag{6}$$

We then use Eqs. 2, 3 to substitute for $\frac{dN}{dt}$ and $\frac{dP}{dt}$ yielding

$$\frac{dN_p}{dt} = \frac{P(N_f + N_u - N_r - kN) - N(P_u - P_r - kP)}{P^2}. \tag{7}$$

This can be solved for the nitrogen fixation rate,

$$N_f = P\frac{dN_p}{dt} + P_r\left(\frac{N_r}{P_r} - N_p\right) + P_u\left(N_p - \frac{N_u}{P_u}\right). \tag{8}$$

If phosphorus release, P_r, is small or in proportion to N_r, then the second term of Eq. 8 is small and can be neglected. If the cell takes up material from the environment which is

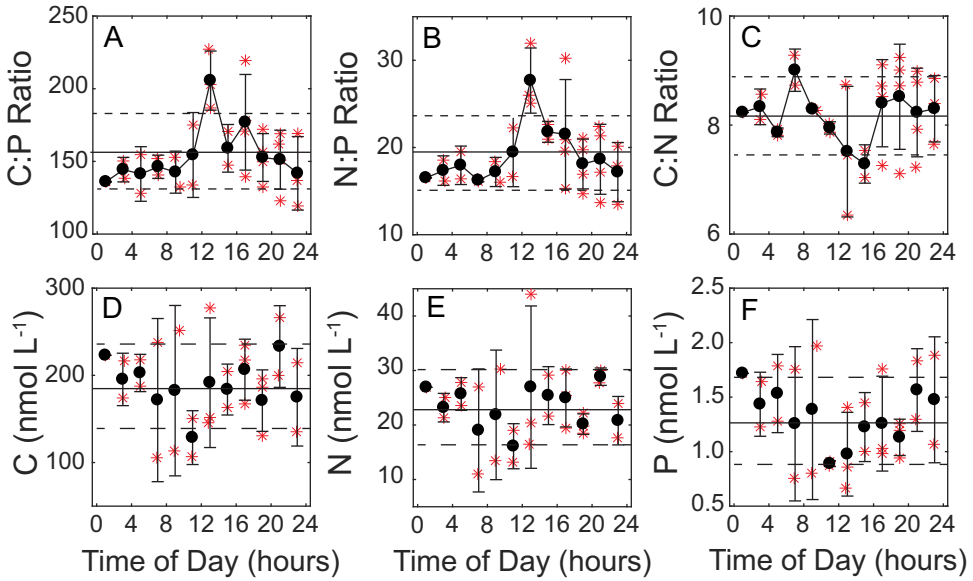

Fig. 3. Elemental stoichiometry over the diurnal cycle, 20−200 μm size class: these six plots show the stoichiometric shifts attributed to large nitrogen fixers over a full photoperiod. Here, $t = 0$ is midnight local time. The C : P ratio (**A**), N : P ratio (**B**), and C : N ratio (**C**), are displayed in the top three plots. Black circles (•) represent averages over 2 h intervals centered on odd numbered hours and are connected by a solid black interpolant to show the diel oscillation more clearly. Stars (∗) represent individual samples. Error bars are the standard deviation of these measurements. The horizontal lines are the mean and one standard deviation above and below the mean for all of the data in the plot. Nitrogen and carbon fixation increase during the morning, leading to a maximum in the N : P and C : P ratios during daylight hours. Imbalances between the carbon and nitrogen fixation would lead to a morning maximum and an evening minimum in the C : N ratio. The carbon concentration (**D**), nitrogen concentration (**E**), and phosphorus concentration (**F**) are displayed in the bottom three plots. The absolute concentrations suggest a daily minimum prior to the maximum found in the N : P and C : P ratios. [Color figure can be viewed at wileyonlinelibrary.com]

either the same or depleted in nitrogen relative to its composition, the third term in Eq. 8 is greater than or equal to zero. This is an implementation of the assumptions discussed in the previous section. Thus, we write

$$N_f \geq P\frac{dN_p}{dt}. \tag{9}$$

The average daily fixation rate, denoted $\langle\rangle$, can thus be expressed by the inequality

$$\langle N_f\rangle \geq \int_{t_1}^{t_2} P\frac{dN_p}{dt}dt, \tag{10}$$

where $t_2 - t_1 < 24$ h. Unlike N : P, N_p, the measured concentrations of C, N, and P over the diel cycle (Fig. 3D–F) are lower bound estimates, have large statistical errors and are influenced by unquantified physical processes. Thus, we assume that the actual concentration of P has a small fluctuation over the diel cycle, or that the changes in P are not related to $\frac{dN_p}{dt}$. This allows us to average P and move it outside the integral,

$$\langle N_f\rangle \geq \langle P\rangle\int_{t_1}^{t_2}\frac{dN_p}{dt}dt. \tag{11}$$

Using the fundamental theorem of calculus, we can write the integral of the derivative of N_p in terms of its values at an initial time t_1 and a second time t_2,

$$\int_{t_1}^{t_2}\frac{dN_p}{dt}dt = N_p(t_2) - N_p(t_1). \tag{12}$$

We now set the initial time, t_1, so that N_p is at its minimum,

$$N_p(t_1) = (N_p)_{min}, \tag{13}$$

and t_2 so that N_p is at its maximum,

$$N_p(t_2) = (N_p)_{max}. \tag{14}$$

Combining Eqs. 10-14 yields the operational form,

$$\langle N_f\rangle \geq \langle P\rangle\left((N_p)_{max} - (N_p)_{min}\right). \tag{15}$$

We have now derived a lower bound on the average nitrogen fixation rate based solely on PN and PP measurements of a discrete size class.

Mortality rate

If the system is in steady state over the diurnal cycle, then we can use our estimate for the nitrogen fixation rate by averaging over Eq. 2 while assuming uptake and release are small,

$$\left\langle\frac{dN}{dt}\right\rangle = \langle N_f\rangle - \langle kN\rangle. \tag{16}$$

If the mortality rate k and nitrogen concentration are not correlated, this equation reduces to

Table 1. Measured quantities, 20–200 μm size fraction: this table contains all of the values required by the equations presented in the "Methods" section. The Range column contains the time windows used to calculate the minimum or maximum value.

Ratio	Range (h)	Minimum value	Range (h)	Maximum value	Range
N : P	0–6	17.4 ± 1.5	12–14	27.7 ± 2.0	10.2 ± 1.9
C : P	0–6	141.5 ± 10.8	12–14	205.6 ± 20.3	64.2 ± 5.0
C : N	14–16	7.3 ± 0.4	6–8	9.0 ± 0.39	1.7 ± 0.86
Element	C (nmol L^{-1} d^{-1})	N (nmol L^{-1} d^{-1})	P (nmol L^{-1} d^{-1})		
Concentration	200 ± 50	25 ± 7	1.3 ± 0.4		

$$\left\langle \frac{dN}{dt} \right\rangle = \langle N_f \rangle - \langle k \rangle \langle N \rangle \tag{17}$$

which can be solved in steady state to find

$$\langle k \rangle = \frac{\langle N_f \rangle}{\langle N \rangle}. \tag{18}$$

We have an estimate for $\langle N_f \rangle$ from the previous section and an estimate for $\langle N \rangle$ so we can calculate the average growth or mortality rate.

Phosphate uptake

Under the same set of assumptions, we can solve for $\langle P_u \rangle$ by substituting into Eq. 3 and then averaging. This yields the expression

$$\langle P_u \rangle = \langle kP \rangle = k \langle P \rangle, \tag{19}$$

under the assumption that mortality is not correlated with elemental concentration.

Carbon fixation

We have no independent constraints on the respiration rate relative to carbon fixation, so we define

$$\tilde{C}_f = C_f - C_r \tag{20}$$

which is the minimum carbon fixation rate since respiration by definition is always positive. We assume that the uptake of organic carbon is small, and the release of organic carbon is included in C_r. Making the same steady state approximation and averaging yields

$$\langle \tilde{C}_f \rangle \geq k \langle C \rangle. \tag{21}$$

We have an equation for k and data for $\langle C \rangle$ so we can estimate the net carbon fixation rate.

Results

Rates from diel stoichiometry measurements in the field

Data for all sampling times is condensed onto a single diurnal cycle in Fig. 3, where local sunrise was $\approx$ 06:00 h and local sunset at $\approx$ 19:00 h. In doing so, we find an emergent and robust diel cycle in the C : P and N : P ratios while the C : N ratio exhibits a more cryptic periodicity (*see* Fig. 3). Interestingly, the absolute concentrations of C, N, and P show a mid-morning minima a couple hours prior to the maxima found in the N : P and C : P ratios. It is important to note, however, that the variance of individual C, N, and P concentrations approaches that of the entire respective data sets. These fluctuations are not robust. Additionally, losses (approximately 10–20%) of material from emptying the cod end of the plankton net are unquantified, so time points are a lower-bound estimate.

All three of these fluctuations can be understood in terms of the diurnal cycle. Following sunrise, rates of both net C and N fixation should exceed P assimilation, causing both the C : P ratio and the N : P ratios to increase until C and N fixation rates slow or cease. At this point, continued P acquisition relaxes both ratios back to their starting points. Trends in the change of C and N concentrations closely track one another (Fig. 3D,E); however, the C : N ratio declines significantly over the photoperiod (from a peak of 9.0 at 07:00 HST to a minimum of 7.2 at 16:00 HST), suggesting that net N fixation rates exceed C fixation relative to a mean molar ratio of 8.2 over the light phase of the diurnal cycle.

An estimate for the minimum, maximum, and average values for the stoichiometric ratios as well as estimates for the lower bound of the average concentrations of N, P, and C in this size fraction are included in Table 1. Notably, the long filtration times inherent to this method, variability in the homogeneity of concentrate used for replicate samples, and variability between successive days lead to large errors in absolute elemental concentrations. This is a novel method and there is great potential to reduce error as part of future efforts.

Combining Eqs. 14, 17, 18, and 20 with the values found in Table 1 allows us to calculate biogeochemical rates in our size class. We find a nitrogen fixation rate of 13 ± 5 nmol L^{-1} d^{-1} along with estimates for growth, mortality, phosphorus uptake, and carbon fixation (*see* Table 2). These rates are all derived from the robust diel fluctuations found in the elemental ratios between C, N, and P. We can also generate a continuous estimate for nitrogen fixation by applying Eq. 9 to our time series of N_p. All pairs of N_p measurements taken between 1 h and 3 h in time-of-day were used to estimate the local nitrogen fixation rate (stars in Fig. 4). These sets were then averaged as they sort well in 2 h time windows.

Table 2. Derived rates, 20–200 μm size fraction: this table contains all of the values derived from the measured changes in elemental stoichiometry as presented in the "Methods" section. It is important to note that all calculated quantities represent a lower bound and that bracketed quantities, $\langle\square\rangle$, represent the diurnal average.

Quantity	Symbol	Equation	Value	Units
N fixation	$\langle N_f \rangle$	$\langle P \rangle \left((N_p)_{max} - (N_p)_{min} \right)$	13.0 ± 5.0	nmol L^{-1} d^{-1}
Growth/mortality	$\langle k \rangle$	$\frac{\langle N_f \rangle}{\langle N \rangle}$	0.5 ± 0.25	d^{-1}
P uptake	$\langle P_u \rangle$	$\langle k \rangle \langle P \rangle$	7 ± 4	nmol L^{-1} d^{-1}
Carbon fixation	$\langle \bar{C}_f \rangle$	$\langle k \rangle \langle C \rangle$	100 ± 50	nmol L^{-1} d^{-1}

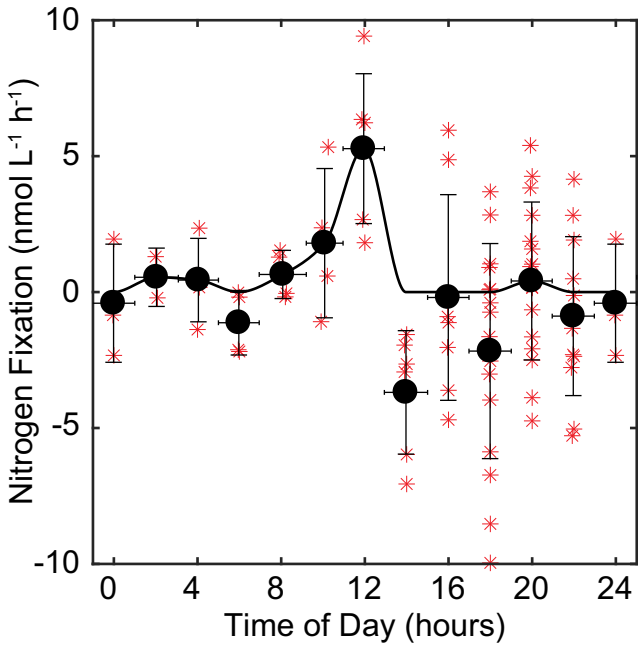

Fig. 4. Continuous estimate from stoichiometry: stars are individual estimates of local nitrogen fixation rate based on the difference of two individual stoichiometric measurements. The black symbols represent the mean in each 2 h time window. All averages below zero are due to phosphorus uptake. A cubic interpolant (solid line) is used to estimate the continuous nitrogen fixation rate. The interpolant was forced to be greater than or equal to zero. [Color figure can be viewed at wileyonlinelibrary.com]

A continuous estimate for nitrogen fixation was then made by interpolating the average values (Fig. 4). This method will generate negative estimates for the nitrogen fixation rate when the ratio decreases due to uptake of phosphorus. Thus, for the continuous estimate, we set all estimates which fell below zero to zero as nitrogen fixation cannot be negative. We will now compare the bulk estimates of nitrogen fixation to culture and contextual field measurements. We will use the continuous estimate for comparison with coincident nitrogen fixation measurements from nitrogen isotopes.

Rates from diel measurements of *Trichodesmium* cultures

Our method can be straightforwardly applied in laboratory cultures, where the nitrogen fixation rate can additionally be determined both through proxies (e.g., acetylene reduction assay [ARA]) and through mass balance. As described in the "Methods" section, duplicate cultures of exponential phase *Trichodesmium* IMS101 were grown on a 12 : 12 light : dark cycle and particulate elements and ARA were measured at 2-h intervals. Data from these experiments is shown in Fig. 5.

The stoichiometric ratios measured in the laboratory show the same oscillatory patterns seen in the field, albeit with a phase shift likely related to sinusoidal vs. square light cycles. In the field, the peak in both N : P and C : P ratios occurs near midday when light intensity is highest. In the laboratory, both of these ratios peak near the end of the day, which is consistent with the constant illumination during daylight hours experienced by these cultures. Consistent with the field, N : P and C : P peak during daytime and the C : N ratio also experiences a daytime minimum. This drop in C : N could also be related to respiration or exudation of carbon rich compounds.

These experiments provide an important test of the underlying assumptions in our model. Although we find that the N : P ratio fluctuates in the experiment like we predict, this was not a forgone conclusion. Diel oscillations in the uptake rates of phosphorus could have easily destroyed the predicted N : P fluctuations, and put our interpretation in doubt. These experiments strongly support our interpretation that changes in N : P are due to nitrogen fixation.

Rate measurements for these culture experiments are shown in Table 3. We find good agreement between the ratio-based (22 ± 10 μmol L^{-1} d^{-1}) and mass balance (20 ± 2 μmol L^{-1} d^{-1}) approach to measurement of net N accumulation in *Trichodesmium* cultures. Rates based on ARA are approximately 2× higher, consistent with the assumption that ARA is a proxy for gross nitrogen fixation and will include production of dissolved inorganic and organic N (Mulholland et al. 2004).

Consistence with contextual field and laboratory measurements

We have also compared our findings to published rate measurements and to complementary in situ data. We find that the bulk rate of nitrogen fixation for the large diazotrophs predicted from the stoichiometric model (13.4 ± 5 nmol L^{-1} d^{-1}) is within the range (8.6 ± 5.6 nmol L^{-1} d^{-1}) found in a similar

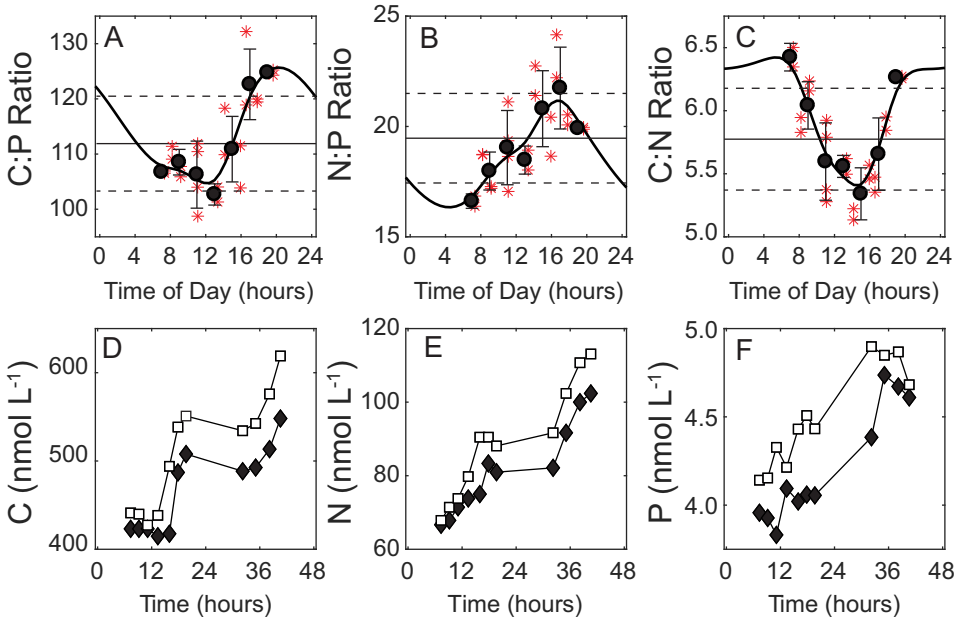

Fig. 5. Elemental stoichiometry for *Trichodesmium* cultures over the diurnal cycle: these six plots show the stoichiometric shifts in the laboratory cultures of *Trichodesmium* condensed on a diel cycle (plots **A**–**C**) and over the 2 d time course of the experiment (plots **D**–**F**). Plots **A**–**C** represent all data condensed on a diel cycle as in Fig. 3. Black circles (•) represent averages over 2 h intervals centered on odd numbered hours. Stars (∗) represent individual samples. Error bars are the standard deviation of these measurements. The horizontal lines are the mean and one standard deviation above and below the mean for all of the data in the plot. The C : P ratio (**A**), N : P ratio (**B**), and C : N ratio (**C**) are displayed in the top three plots. Nitrogen and carbon fixation occur during daylight, leading to a maximum in the N : P and C : P ratios during daylight hours. Imbalances between the carbon and nitrogen fixation would lead to a morning maximum and an evening minimum in the C : N Ratio. The carbon concentration (**D**), nitrogen concentration (**E**), and phosphorus concentration (**F**) are displayed in the bottom three plots (**D**–**F**). The full time course of both 2-d experiments is displayed (represented by □ and ◆, respectively). Consistent with our assumptions, both N and P are monotonically increasing, with P uptake during the night. Respiration can be seen in the nighttime decrease in total carbon. [Color figure can be viewed at wileyonlinelibrary.com]

Table 3. Derived rates from *Trichodesmium* experiments: this table contains all of the values derived from the measured changes in elemental stoichiometry for the *Trichodesmium* experiments. The ratio methods are the same as those presented in the "Methods" section. The cultures allow us to also use mass balance (total N generated) and direct methods (acetylene reduction, ARA). All three of these methods agree with one another, with ARA being about twice as large because it is a gross rather than a net measurement. The absolute rates are much larger because the culture is much more concentrated than in the field.

Quantity	Method	Equation	Value	Units
N fixation	Ratio	$\langle P \rangle \left((N_p)_{max} - (N_p)_{min} \right)$	22 ± 10	μmol L^{-1} d^{-1}
	Mass balance	$(N_{max} - N_{min})$	20 ± 2	μmol L^{-1} d^{-1}
	Acetylene reduction	N/A	47 ± 5	μmol L^{-1} d^{-1}
Growth	Ratio	$\frac{\langle N_t \rangle}{\langle N \rangle}$	0.26 ± 0.11	d^{-1}
P uptake	Ratio	$\langle k \rangle \langle P \rangle$	1.1 ± 0.5	μmol L^{-1} d^{-1}
C fixation	Ratio	$\langle k \rangle \langle C \rangle$	128 ± 56	μmol L^{-1} d^{-1}

mesoscale feature in the NPSG (Fong et al. 2008), and more importantly within the range (0.5–20.0 nmol L^{-1} d^{-1}) attained during 9 yr of nitrogen fixation measurements at station ALOHA (Böttjer et al. 2017). Moreover, the derived diazotrophic growth rate of 0.5 ± 0.25 d^{-1} for this size fraction is consistent with estimates from laboratory cultures of 0.67 d^{-1} and 0.77 d^{-1} for DDAs (Villareal 1989, 1990) and is expected to be lower due to the *Trichodesmium* in our samples (maximum growth rates 0.3 d^{-1}, Breitbarth et al. 2008). Comparing C based stocks and rates, we find that (1) the concentration of total PC measured from the ships flow-through systems (3.4 ± 0.6 μmol L^{-1}) is consistent with PC measured from CTD-rosette collections at 5 m (3.8 ± 0.8 μmol L^{-1}, $n = 4$), and (2) the average carbon in the 20–200 μm size-fraction (200 nmol L^{-1}) accounts for 6% of total PC, a value within the range of the contribution of large diazotrophs to total suspended PC at Station ALOHA, 6–11% as per (Letelier and Karl 1996) and last (3) the mean diazotrophic C fixation rates estimated here,

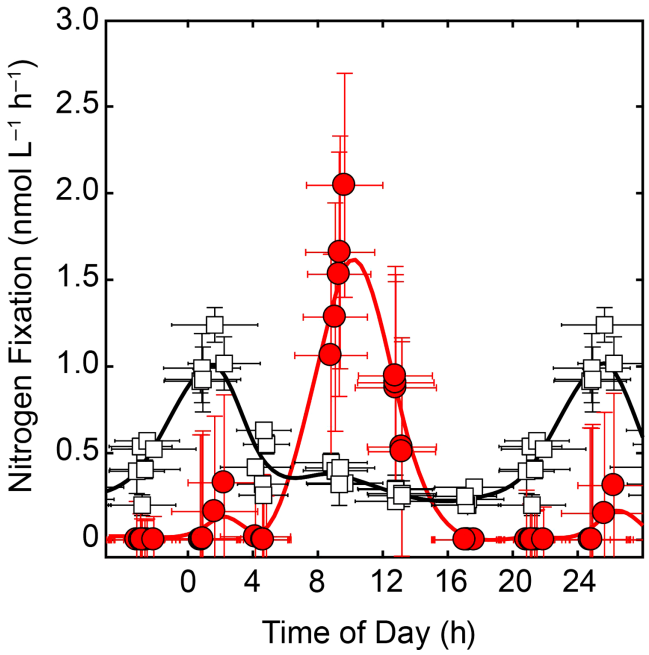

Fig. 6. Comparison of measured $^{15}N_2$ fixation (□) rates with those diagnosed for the 20–200 mm size fraction from elemental ratios (red filled circles). The ^{15}N derived curve peaks at nighttime, likely due to *Crocosphaera* (Wilson et al. 2017) while the large size fraction peaks during the daytime. This is consistent with solar irradiation driving nitrogen fixation in DDAs and *Trichodesmium*. The solid curves are smoothing interpolants of the underlying data, designed to show the diel trends more clearly. [Color figure can be viewed at wileyonlinelibrary.com]

100 ± 50 nmol C L^{-1} d^{-1}, are 7–8% of ^{14}C based C fixation rates from this same cruise (16.1 ± 1.5 mg C m^{-3} d^{-1}, White et al. 2017), a contribution again consistent with inputs via large diazotrophs measured by (Letelier and Karl 1996) on the order of 5%. We recognize the large ranges in some of this data, but find it important that none of it falsifies our results.

Making a few simplifying assumptions, we can also compare independently measured cell counts to our results. The concentration of *Richelia* heterocysts and *Trichodesmium* cells were directly measured. Hence, *Richelia* cell abundance can be estimated by multiplying heterocyst concentrations by 5, i.e., assuming five cells per filament (Villareal 1989) and *Richelia* carbon can then be estimated assuming 10 pg C cell^{-1} (Luo et al. 2012). *Trichodesmium* carbon is simply estimated assuming 300 pg C cell^{-1} (Luo et al. 2012). Finally, given that we found most DDA's to consist of 1–4 *Richelia* per host, we can conservatively estimate host concentrations to be a quarter of the heterocyst concentrations and diatom host C can be calculated using the minimum C content for *Rhizosolenia*, 14 ng C cell^{-1} reported by (Poulton et al. 2009). By this approach, we estimate the carbon concentration in large diazotrophs to be 100−300 nmol C L^{-1} based on microscopy, where the range represents the uncertainty in symbiont to host ratio. This estimate is consistent with our carbon measurement of 200 ± 50 nmol C L^{-1}, however, it is of course prone to error in assumed carbon quotas and diatom-symbiont ratios. These calculations only confirm that cell-based estimates of PC derived from 10-L volumes and the size-fractionated C measurements are of similar magnitude.

Comparison with diel ^{15}N nitrogen fixation time series

During our field campaign, nitrogen fixation was also measured across the diurnal cycle (Wilson et al. 2017) using the ^{15}N isotope tracer technique (Mohr et al. 2010; Wilson et al. 2012). Details of these measurements and their relation to diazotrophic community structure can be found in Wilson et al. (2017). These measurements were conducted using water collected from 15 m; were made at approximately 4 h intervals; and were conducted in deck board incubations, under simulated light conditions. Nitrogen fixation rate measurements range from 0.2 nmol L^{-1} h^{-1} to 1.2 nmol L^{-1} h^{-1} with low values occurring during the daylight and peak values found between midnight and dawn. The nitrogen fixation estimates from stoichiometry and isotopes are plotted together in Fig. 6. To make the data comparable, our method and model were resampled over the incubation time windows used for the isotope measurements. Although the average nitrogen fixation measured with traditional methods is comparable to that inferred from stoichiometry, the peak fixation occurs at night for the isotope method whereas stoichiometry predicts a strong peak during the day. The nighttime peak found by traditional methods is consistent with the large amount of *Crocosphaera* found during the cruise (Wilson et al. 2017) and *Crocosphaera* are known to fix nitrogen at night (Zehr 2011). The nitrogen fixation time series inferred from stoichiometry has no nighttime peak because *Crocosphaera* is not concentrated by sampling the >20 μm size fraction. However, it is unclear why the daytime nitrogen fixation peak inferred from stoichiometry is not present in the isotopic time series (Fig. 6).

Discussion

It is extremely difficult to measure the chemical flux through the surface ocean when it is in steady state. Isotope tracer incubation studies overcome this issue by adding an out-of equilibrium tracer which acts like a steady state variable. These techniques are broadly applied to measure rates like primary production and nitrogen fixation (Steeman-Nielsen 1952; Fuhrman and Azam 1982; Hama et al. 1983; Capone 1993; Fong et al. 2008). However, they all suffer from bottle and handling effects, such that in vitro measurements can differ significantly from in vivo approaches. We present an alternative approach for estimating diazotrophic rates via diurnal changes in size-fractionated elemental stoichiometry. Our approach comes with its own set of assumptions and is complementary to current techniques. How does our approach fit in the context of other measurements?

It remains unclear what causes the discrepancy between daytime nitrogen fixation rates as estimated by stoichiometric changes when compared to isotope tracer techniques. If our interpretation of the elemental data is correct, then we expect that differences in sample handling are the cause. Water for traditional tracer-based nitrogen fixation measurements was sampled from a Niskin bottle (~4 L) at 15 m depth whereas water for the elemental analysis was taken from the flow-through system (~1000 L) closer to the surface (5–7 m). One possibility is that small bottle samples underestimate the bulk concentration of the large size fraction. It is well known that settling can strongly bias results when a Niskin bottle is not fully drained, leading to underestimates of bulk particulates by up to 70% (Gardner 1977). Recent work showed that 1 h of settling time was sufficient to render all particles greater than 16 μm in diameter undetectable because they sank below the Niskin spout (Suter et al. 2017). Floating cells would cause a similar problem. These particle migration effects should occur inside the incubation vessel as well, and would lead to the concentration of large cells against the walls of the incubation vessel. Under this scenario, bulk nitrogen fixation during our cruise may be best estimated by adding the results of the two methods. This would yield approximately 25 nmol L^{-1} d^{-1}. Future work and replication is required to determine both if this is an endemic issue and its average magnitude. Here, we suggest that bottle incubations may have underestimated nitrogen fixation by a factor of two.

Another possibility is that the underlying assumptions behind our calculations are incorrect. Large fluctuations in the ratio of N : P due to variable uptake ratios over the course of a day or trophic transfer could nullify our results. We believe that neither of these possibilities is likely at our field site for reasons that we describe below. First, we consider whether changes in the N : P ratio over the diel cycle could be due to changes in relative uptake and release of nitrogen and phosphorus over the diel cycle. Phytoplankton can exhibit diel patterns in the efficiency with which they assimilate N and P due to energy-requirements of transport and variable affinities for N vs. P (Rhee and Gotham 1980). Under P limitation, experiments have shown large increases in N : P during daylight in freshwater diatoms (Rhee and Gotham 1980). However, under nitrogen limitation, the excursion would be expected to have the opposite sign, and be of much smaller magnitude. Existing experimental evidence suggests that these excursions do not occur under nitrogen limitation (Lopez et al. 2016). In the NPSG, phytoplankton are severely nitrogen limited which can be seen in the environmental ratio of inorganic N : P. This ratio is less than 0.5, as opposed to the Redfield ratio which is closer to 16 (Karl and Church 2014). Additionally, the absolute concentration of free nitrogen is approximately 1% of nitrogen contained in biomass. If our observed fluctuation was uniform across all phytoplankton, we would expect environmental inorganic nitrogen to increase to over 50 times its observed concentration during the night. Combined, this evidence strongly suggests that diel patterns of the uptake and release of nitrogen are not capable of explaining our observed fluctuations in the N : P ratio.

Another possibility is that there is a trophic transfer of nitrogen relative to phosphorus into our size class through the consumption of diazotroph-derived nitrogen rich organic matter during the day. This mechanism is hard to justify because small nitrogen fixers make up less than 5% of the total biomass of small phytoplankton and large cell-sized organisms would be poor competitors for dissolved organic nitrogen or if predators, unlikely to efficiently prey on such rare particles. Additionally, the predation would have to occur during mid-morning when we observe increases in the N : P ratio. However, measured consumption rates of small phytoplankton peak during the night (Ribalet et al. 2015). Diurnal fluctuations in the biases of our size fraction could also play a role, but we have no mechanism to quantify these.

The NPSG provides the ideal situation for assessments of diurnal cycles, as the surface ocean is generally thought to be close to steady state (Karl and Church 2014) and the strong dependence of photosynthesis and diazotrophy on solar forcing lead to persistent diurnal cycles in major elemental cycles. Estimates of the diurnal cycle in PC concentrations have been used in this way to estimate bulk primary production (Stramska and Dickey 1992; Walsh et al. 1995; Johnson et al. 2006). Changes in the absolute concentration of a particular element, however, can be difficult to detect due to sampling constraints or nonexistent if net growth is balanced by net loss (Ribalet et al. 2015). For cellular growth models, this is overcome by normalizing each measurement to the total cell number and modeling the dynamics of the probability density function (Sosik et al. 2003; Ribalet et al. 2015). We take a similar approach by normalizing to the phosphorus concentration and analyzing the dynamics of the stoichiometric ratios. The absolute quantities come into the equations only in their time average. These methods generate in situ diazotrophic rate estimates that can be compared to parallel bottle-based measurements. They can be used together to better understand the contributions of large diazotrophs to elemental cycling in oligotrophic ocean regimes.

This method has multiple avenues for expansion and improvement. Future iterations must improve the resolution on absolute concentrations. We will move from an open-air plankton net, to a system which relies on in-line mesh filters and eliminates concentrate loss. Our analysis can be used with any system which measures the PC : PN : PP of a series of size fractions across time. With the proper advances, we envision a semi-continuous record of size class dependent biogeochemical rates, in addition to the biological rates found with flow-cytometry (Sosik et al. 2003; Ribalet et al. 2015).

Conclusion

Real time measurements of diurnal change in dissolved nutrients, particle composition, and concentration have generated great progress in our understanding of biogeochemical fluxes and their variability (Walsh et al. 1995; Johnson et al. 2006; Ribalet et al. 2015). We use diurnal changes in the stoichiometric ratios of C, N, P to estimate a set of biogeochemical rates, particularly nitrogen fixation. We find that large nitrogen fixing organisms in an anticyclonic feature in the NPSG fix upward of 13 nmol NL^{-1} d^{-1}. This is comparable to bulk surface measurements from similar features and is consistent with observations of elevated diazotroph biomass during this cruise. This technique has the potential to greatly enhance our ability to measure nitrogen fixation and assess its role in driving carbon sequestration in the deep sea.

References

Böttjer, D., J. E. Dore, D. M. Karl, R. M. Letelier, C. Mahaffey, S. T. Wilson, J. Zehr, and M. J. Church. 2017. Temporal variability of nitrogen fixation and particulate nitrogen export at Station ALOHA. Limnol. Oceanogr. **62**: 200–216. doi:10.1002/lno.10386

Breitbarth, E., J. Wohlers, J. Kläs, J. LaRoche, and I. Peeken. 2008. Nitrogen fixation and growth rates of *Trichodesmium* IMS-101 as a function of light intensity. Mar. Ecol. Prog. Ser. **359**: 25–36. doi:10.3354/meps07241

Capone, D. G. 1993. Determination of nitrogenase activity in aquatic samples using the acetylene reduction procedure, p. 621–631. *In* P. F. Kemp, B. F. Sherr, E. B. Sherr, and J. J. Cole [eds.], Handbook of methods in aquatic microbial ecology. Lewis Press.

Capone, D. G., J. A. Burns, J. P. Montoya, A. Subramaniam, C. Mahaffey, T. Gunderson, A. F. Michaels, and E. J. Carpenter. 2005. Nitrogen fixation by *Trichodesmium* spp.: An important source of new nitrogen to the tropical and subtropical North Atlantic Ocean. Global Biogeochem. Cycles **19**: GB2024. doi:10.1029/2004GB002331

Chen, Y., J. P. Zehr, and M. Mellon. 1996. Growth and nitrogen fixation of the diazotrophic filamentous nonheterocystous cyanobacterium *Trichodesmium* sp. IMS 101 in defined media: Evidence for a circadian rhythm. J. Phycol. **32**: 916–923. doi:10.1111/j.0022-3646.1996.00916.x

Claustre, H., Y. Huot, I. Obernosterer, B. Gentili, D. Tailliez, and M. Lewis. 2007. Gross community production and metabolic balance in the South Pacific Gyre, using a non intrusive bio-optical method. Biogeosci. Discuss. **4**: 3089–3121. doi:10.5194/bg-5-463-2008

Dabundo, R., M. F. Lehmann, L. Treibergs, C. R. Tobias, M. A. Altabet, P. H. Moisander, and J. Granger. 2014. The contamination of commercial $^{15}N_2$ gas stocks with ^{15}N–labeled nitrate and ammonium and consequences for nitrogen fixation measurements. PLoS One **9**: e110335. doi:10.1371/journal.pone.0110335

Fong, A. A., D. M. Karl, R. Lukas, R. M. Letelier, J. P. Zehr, and M. J. Church. 2008. Nitrogen fixation in an anticyclonic eddy in the oligotrophic North Pacific Ocean. ISME J. **2**: 663–676. doi:10.1038/ismej.2008.22

Fuhrman, J. A., and F. Azam. 1982. Thymidine incorporation as a measure of heterotrophic bacterioplankton production in marine surface waters: Evaluation and field results. Mar. Biol. **66**: 109–120. doi:10.1007/BF00397184

Gardner, W. D. 1977. Incomplete extraction of rapidly settling particles from water samplers. Limnol. Oceanogr. **22**: 764–768. doi:10.4319/lo.1977.22.4.0764

Geider, R., and J. LaRoche. 2002. Redfield revisited: Variability of C:N:P in marine microalgae and its biochemical basis. Eur. J. Phycol. **37**: 1–17. doi:10.1017/S0967026201003456

Hama, T., T. Miyazaki, Y. Ogawa, T. Iwakuma, M. Takahashi, A. Otsuki, and S. Ichimura. 1983. Measurement of photosynthetic production of a marine phytoplankton population using a stable ^{13}C isotope. Mar. Biol. **73**: 31–36. doi:10.1007/BF00396282

Hunter-Cevera, K. R., M. G. Neubert, A. R. Solow, R. J. Olson, A. Shalapyonok, and H. M. Sosik. 2014. Diel size distributions reveal seasonal growth dynamics of a coastal phytoplankter. Proc. Natl. Acad. Sci. USA **111**: 9852–9857. doi:10.1073/pnas.1321421111

Janson, S., B. Bergman, E. J. Carpenter, S. J. Giovannoni, and K. Vergin. 1999. Genetic analysis of natural populations of the marine diazotrophic cyanobacterium *Trichodesmium*. FEMS Microbiol. Ecol. **30**: 57–65. doi:10.1111/j.1574-6941.1999.tb00635.x

Johnson, K. S., L. J. Coletti, and F. P. Chavez. 2006. Diel nitrate cycles observed with in situ sensors predict monthly and annual new production. Deep-Sea Res. Part I Oceanogr. Res. Pap. **53**: 561–573. doi:10.1016/j.dsr.2005.12.004

Karl, D. M., J. E. Dore, D. V. Hebel, and C. Winn. 1991. Procedures for particulate carbon, nitrogen, phosphorus and total mass analyses used in the US-JGOFS Hawaii Ocean Time-Series program, p. 71–77. *In* D. C. Hurd and D. Spencer [eds.], Marine particles: Analysis and characterization. American Geophysical Union.

Karl, D. M., and R. Lukas. 1996. The Hawaii Ocean Time-Series (HOT) program: Background, rationale and field implementation. Deep-Sea Res. Part II Top. Stud. Oceanogr. **43**: 129–156. doi:10.1016/0967-0645(96)00005-7

Karl, D. M., R. Letelier, L. Tupas, J. Dore, J. Christian, and D. Hebel. 1997. The role of nitrogen fixation in biogeochemical cycling in the subtropical North Pacific Ocean. Nature **388**: 533–538. doi:10.1038/41474

Karl, D. M., M. J. Church, J. E. Dore, R. M. Letelier, and C. Mahaffey. 2012. Predictable and efficient carbon sequestration in the North Pacific Ocean supported by symbiotic nitrogen fixation. Proc. Natl. Acad. Sci. USA **109**: 1842–1849. doi:10.1073/pnas.1120312109

Karl, D. M., and M. J. Church. 2014. Microbial oceanography and the Hawaii Ocean Time-series programme. Nat. Rev. Microbiol. **12**: 699–713. doi:10.1038/nrmicro3333

Letelier, R. M., and D. M. Karl. 1996. Role of *Trichodesmium* spp. in the productivity of the subtropical North Pacific Ocean. Mar. Ecol. Prog. Ser. **133**: 263–273. doi:10.3354/meps133263

Lomas, M. W., D. A. Bronk, and G. van den Engh. 2011. Use of flow cytometry to measure biogeochemical rates and processes in the ocean. Ann. Rev. Mar. Sci. **3**: 537–566. doi:10.1146/annurev-marine-120709-142834

Lopez, J. S., N. S. Garcia, D. Talmy, and A. C. Martiny. 2016. Diel variability in the elemental composition of the marine cyanobacterium *Synechococcus*. J. Plankton Res. **38**: 1052–1061. doi:10.1093/plankt/fbv120

Luo, Y.-W., and others. 2012. Database of diazotrophs in global ocean: Abundance, biomass and nitrogen fixation rates. Earth Syst. Sci. Data **4**: 47–73. doi:10.5194/essd-4-47-2012

McInnes, A. S., A. K. Shepard, E. J. Raes, A. M. Waite, and A. Quigg. 2014. Simultaneous quantification of active carbon-and nitrogen-fixing communities and estimation of fixation rates using fluorescence in situ hybridization and flow cytometry. Appl. Environ. Microbiol. **80**: 6750–6759. doi:10.1128/AEM.01962-14

Mohr, W., T. Grosskopf, D. Wallace, and J. LaRoche. 2010. Methodological underestimation of oceanic nitrogen fixation rates. PLoS One **5**: e12583. doi:10.1371/journal.pone.0012583

Montoya, J. P., M. Voss, P. Kahler, and D. G. Capone. 1996. A simple, high-precision, high-sensitivity tracer assay for N_2 fixation. Appl. Environ. Microbiol. **62**: 986–993. http://aem.asm.org/content/62/3/986.full.pdf+html

Mulholland, M. R., D. A. Bronk, and D. G. Capone. 2004. Dinitrogen fixation and release of ammonium and dissolved organic nitrogen by *Trichodesmium* IMS101. Aquat. Microb. Ecol. **37**: 85–94. doi:10.3354/ame037085

Olson, R. J., A. Shalapyonok, and H. M. Sosik. 2003. An automated submersible flow cytometer for analyzing pico- and nanophytoplankton: FlowCytobot. Deep-Sea Res. Part I Oceanogr. Res. Pap. **50**: 301–315. doi:10.1016/S0967-0637(03)00003-7

Poulton, A. J., M. C. Stinchcombe, and G. D. Quartly. 2009. High numbers of *Trichodesmium* and diazotrophic diatoms in the southwest Indian Ocean. Geophys. Res. Lett. **36**: L15610. doi:10.1029/2009GL039719

Prufert-Bebout, L., H. W. Paerl, and C. Lassen. 1993. Growth, nitrogen fixation, and spectral attenuation in cultivated *Trichodesmium* species. Appl. Environ. Microbiol. **59**: 1367–1375. http://aem.asm.org/content/59/5/1367.full.pdf+html

Rhee, G.-Y., and I. J. Gotham. 1980. Optimum N:P ratios and coexistence of planktonic algae. J. Phycol. **16**: 486–489. doi:10.1111/j.1529-8817.1980.tb03065.x

Ribalet, F., and others. 2015. Light-driven synchrony of *Prochlorococcus* growth and mortality in the subtropical Pacific gyre. Proc. Natl. Acad. Sci. USA **112**: 8008–8012. doi:10.1073/pnas.1424279112

Sosik, H. M., R. J. Olson, M. G. Neubert, A. Shalapyonok, and A. R. Solow. 2003. Growth rates of coastal phytoplankton from time-series measurements with a submersible flow cytometer. Limnol. Oceanogr. **48**: 1756–1765. doi:10.4319/lo.2003.48.5.1756

Steeman-Nielsen, E. 1952. The use of radioactive carbon (^{14}C) for measuring organic production in the sea. ICES J. Mar. Sci. **18**: 117–140. doi:10.1093/icesjms/18.2.117

Stramska, M., and T. D. Dickey. 1992. Variability of bio-optical properties of the upper ocean associated with diel cycles in phytoplankton population. J. Geophys. Res. Oceans **97**: 17873–17887. doi:10.1029/92JC01570

Suter, E. A., M. I. Scranton, S. Chow, D. Stinton, L. Medina Faull, and G. T. Taylor. 2017. Niskin bottle sample collection aliases microbial community composition and biogeochemical interpretation. Limnol. Oceanogr. **62**: 606–617. doi:10.1002/lno.10447

Terry, K. L., J. Hirata, and E. A. Laws. 1985. Light-, nitrogen-, phosphorus-limited growth of *Phaeodactylum tricornutum* Bohlin strain TFX-1: Chemical composition, carbon partitioning, and the diel periodicity of physiological processes. J. Exp. Mar. Biol. Ecol. **86**: 85–100. doi:10.1016/0022-0981(85)90044-9

Villareal, T. A. 1989. Division cycles in the nitrogen-fixing *Rhizosolenia (Bacillariophyceae)-Richelia (Nostocaceae)* symbiosis. Br. Phycol. J. **24**: 357–365. doi:10.1080/00071618900650371

Villareal, T. A. 1990. Laboratory culture and preliminary characterization of the nitrogen-fixing *Rhizosolenia-Richelia* symbiosis. Mar. Ecol. **11**: 117–132. doi:10.1111/j.1439-0485.1990.tb00233.x

Walsh, I. D., S. P. Chung, M. J. Richardson, and W. D. Gardner. 1995. The diel cycle in the integrated particle load in the equatorial Pacific: A comparison with primary production. Deep-Sea Res. Part II Top. Stud. Oceanogr. **42**: 465–477. doi:10.1016/0967-0645(95)00030-T

White, A. E., D. M. Karl, K. Bjorkman, L. J. Beversdorf, and R. M. Letelier. 2010. Production of organic matter by *Trichodesmium* IMS101 as a function of phosphorus source. Limnol. Oceanogr. **54**: 1755. doi:10.4319/lo.2010.55.4.1755

White, A. E., B. Barone, R. M. Letelier, and D. M. Karl. 2017. Productivity diagnosed from the diel cycle of particulate carbon in the North Pacific Subtropical Gyre. Geophys. Res. Lett. **44**: 3752–3760. doi:10.1002/2016GL071607

White, A. E., K. Watkins-Brandt, and M. J. Church. 2018. Temporal variability of *Trichodesmium* and *Richelia* spp. in the North Pacific Subtropical Gyre. Front. Aquat. Microbiol. **5**(27). doi:10.3389/fmars.2018.0002

Wilson, S. T., D. Böttjer, M. J. Church, and D. M. Karl. 2012. Comparative assessment of nitrogen fixation methodologies, conducted in the oligotrophic North Pacific Ocean. Appl. Environ. Microbiol. **78**: 6516–6523. doi:10.1128/AEM.01146-12

Wilson, S. T., and others. 2017. Coordinated regulation of growth, activity and transcription in natural populations of the unicellular nitrogen-fixing cyanobacterium *Crocosphaera*. Nat. Microbiol. **2**: 17118. doi:10.1038/nmicrobiol.2017.118

Zehr, J. P. 2011. Nitrogen fixation by marine cyanobacteria. Trends Microbiol. **19**: 162–173. doi:10.1016/j.tim.2010.12.004

Acknowledgments

The authors thank Tara Clemente for cruise leadership of KOK1507, significant technical support, and particulate phosphorus analysis; Eric Grabowski for analysis of particulate carbon and nitrogen; Katie Watkins-Brandt for all laboratory experiments and subsequent analytical measurements and David Karl for thoughtful comments on the manuscript. The design of field experiments benefited from conversations with Jeffrey Krause and Benjamin Twining. This work was supported by grants from the Simons Foundation (329108, Angelique E. White, Michael J. Follows and David M. Karl; 553242, Christopher L. Follett) and the Gordon and Betty Moore Foundation (3778, Michael J. Follows and 3794, David M. Karl).

Conflict of Interest

None declared.

Submitted 15 September 2017
Revised 12 February 2018
Accepted 14 March 2018

Associate editor: Maren Voss